LBL-12114 c.2
Preprint

Lawrence Berkeley Laboratory
UNIVERSITY OF CALIFORNIA

CHEMICAL BIODYNAMICS DIVISION

Submitted to Solar Energy Materials

SOLAR INDUCED WATER SPLITTING WITH p/n HETEROTYPE PHOTOCHEMICAL DIODES: n-Fe_2O_3/p-GaP

Howard Mettee, John W. Otvos, and Melvin Calvin

January 1981

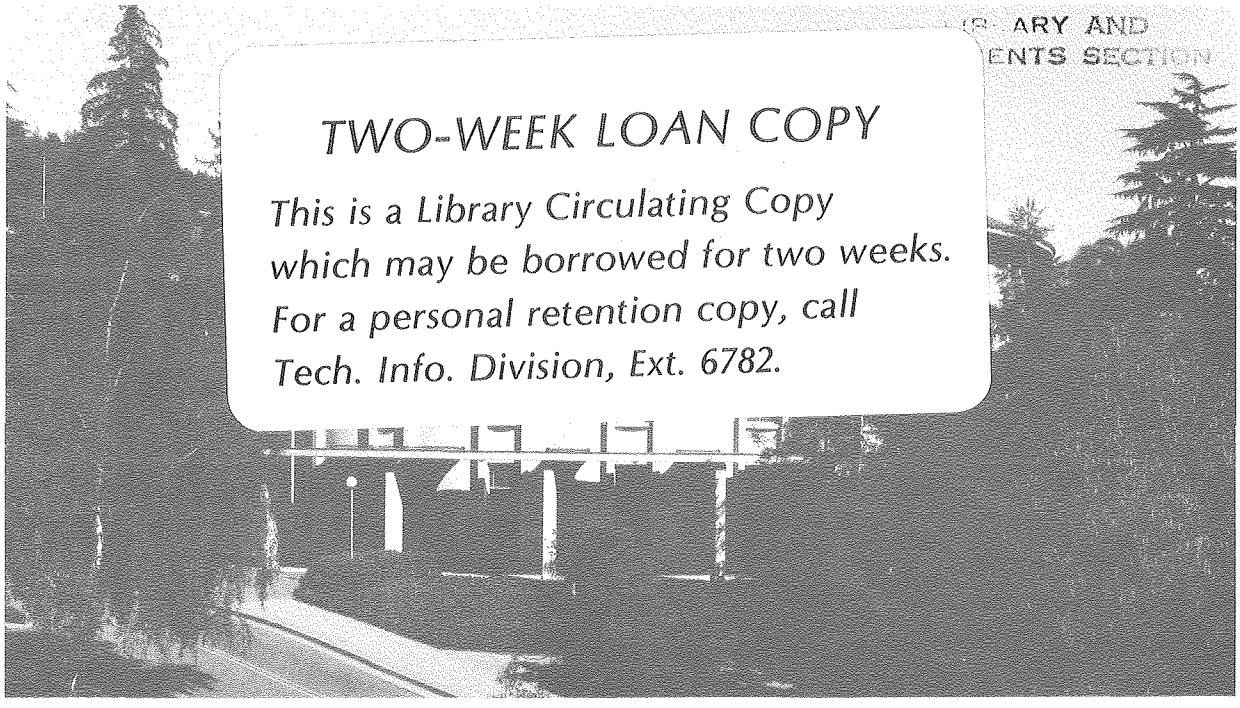

Prepared for the U.S. Department of Energy under Contract W-7405-ENG-48

DISCLAIMER

Solar Induced Water Splitting with p/n Heterotype Photochemical Diodes: n-Fe_2O_3/p-GaP

by

Howard Mettee,* John W. Otvos and Melvin Calvin

Melvin Calvin Laboratory

Lawrence Berkeley Laboratory

University of California

Berkeley, California 94720

*To whom correspondence should be addressed: Department of Chemistry, Youngstown State University, Youngstown, Ohio 44555.

Abstract

A p/n photochemical diode consisting of p-GaP and n-Fe_2O_3 has been assembled in a monolithic unit which, when exposed to visible and near uv radiation in aqueous solution, produces hydrogen in relatively low quantum yields. This unit also splits seawater using incident solar radiation. Both photoelectrode materials showed enhancements of their photo currents when catalysts (RuO_2 on n-Fe_2O_3 and Pt on p-GaP) were deposited on their surfaces. The gases generated at each electrode were mass spectrometrically confirmed as originating from the water.

Introduction

Since the first modern light assisted electrolysis of water using a semiconductor electrode was performed by Fujishima and Honda (1), many materials have been tested which can accomplish this goal (2). Yet none has so far been shown to simultaneously satisfy the obvious requirements of using only visible light, long term stability, operability at near neutral pH's with a practical efficiency and reasonable economies of fabrication.

The p/n photochemical diode cell assembled by Yoneyama et al (3), whose conceptual similarity to photosynthesis has been noted by Nozik (4b) (Fig. 1), is an attractive vehicle with which to conduct water splitting. For the heterotype p/n cells, in which the semiconductor materials used as the photoanode and photocathode are different, a theoretical efficiency estimate as great as 25% has been calculated (2b). Such cells as have actually been assembled, however, not only do not closely approach this efficiency but also include at least one photoelectrode which absorbs in the ultraviolet, have been shown to function only in concentrated acid or base, and use only expensive single crystal materials (3, 4, 5).

It is important to demonstrate that working units designed according to the p/n heterodiode concept can actually be made which operate using only visible light, at close to neutral pH (or preferably in abundant seawater), be reasonably stable and simply fabricated. The photoelectrochemical cell developed in our studies fulfills these criteria, and while its efficiency is still not practical, this characteristic is enhanced by "seeding" the semiconductor surfaces with known H_2 and O_2 generating catalysts.

The diode under consideration consists of a polycrystalline layer of n-Fe_2O_3 oxidized on a thin plate of pure Fe to which has been ohmically attached a thin wafer of Zn-doped p-GaP. Before assembly, each photoelectrode material was separately tested as to its electrochemical behavior before and after the surface catalysts were added. Both of these materials have been characterized by others (6,7).

Figure 2 summarizes the operational characteristics of the combined cell as predicted

using simple semiconductor-electrolyte theory. The elementary requirements are that the valence band of the n-type material must be at a more positive redox potential than the H_2O/O_2 couple, while the conduction band of the p-type material must be at a more negative redox potential than the H^+/H_2 couple (2,8). Also, the photocurrent onset potential of the anode must occur at voltages more negative than that of the cathode in order that a short circuit current flow between them. Band bending (V_B) is calculated here from the flat band potential (V_{fb}), the redox potential (V_R) of the H_2O/O_2 couple at the anode, and the H^+/H_2 couple at the cathode, ($V_B = V_R - V_{fb}$). The Fermi level for the combined system lies between these two couples, and shifts upward on illumination.

Experimental

α-Fe_2O_3 was prepared by the method of Hackerman and Yeh (9), using 99.9985% Puratronic iron produced by Johnson Matthey Chemicals, Ltd., and distributed by the Alpha Division of the Ventron Corporation (Danvers, MA). Zinc doped p-GaP single crystal wafers were obtained from the Cambridge Instrument Company (Monsey, NY), and were sawed perpendicular to the <111> face. This material had a stated carrier concentration of $(4 \pm 1) \times 10^{17}$ and a resistance of 9 ohm-cm.

The occurrence of the onset of the photocurrent at ~. 7V more negative than the flatband potential noted by Butler and Ginley (7) for a similar p-GaP material was not observed in our work, perhaps due to the differences in pH (13 vs. ~ 7).

Separate electrodes of Fe_2O_3 and GaP were prepared by mounting the photoactive material in a Ag-epoxy layer (E-Solder No. 3025, Acme Chemicals, New Haven, CN), which was spread on a wire contacted glass support. An insulating coating of either silicone rubber (Dow Corning, Midland, MI) or ordinary epoxy resin (E·Pox·E, Duro, Cleveland, OH) overcoated with paraffin wax, surrounded the semiconductor so that only its surface made electrical contact with the solution. The GaP wafers were cut into 5 x 10 x 1 mm rectangles with a string saw. The Fe_2O_3 electrodes were made with 5 mm diameter x 1 mm thick discs, oxidized for 14 min in air, and whose mounted faces were scrapped to bare iron.

The combined electrode unit was formed on a 2 mm thick plate of Puratronic iron

65 x 45 mm^2 in area, whose α-Fe_2O_3 layer was formed by heating each side with a Fischer burner for 14 min in air. A 35 mm diameter p-GaP wafer was then mounted on a scrapped end of the plate with Ag-epoxy. The junction, edges and dark side were sealed with a 50:50 mixture of Apiezon W:paraffin wax so that only the two photoelectrode surfaces made electrical contact with the solution.

Figure 3 shows the photoelectrochemical apparatus used to characterize the electrodes. The circuit permits manual control of a known bias voltage as well as other operations not convenient with ordinary potentiostats. The light source was a 1000 W Xe lamp filtered through 10 cm of 10% $CuSO_4$, which passed 340-560 nm. The combined heterodiode was also tested in natural sunlight.

Deposition of the catalytic materials was accomplished in two ways — vacuum or electrochemical. The Vacuum Coating Department (L.B.L.) assisted in depositing thin layers of Pt or p-GaP. Calculated thicknesses of 8, 11 and 14 Å, were estimated by weighing Al foil (target) discs (15 cm radius) next to the electrode before and after deposition of a trace quantity of Pt heated by an electron gun. Since small metallic clusters tend to form under such conditions (10) it was reasoned that this range of nominal thicknesses would not completely cover the semiconductor surface and yet would provide sufficient Pt to exhibit an effect.

Electrolytic depositions were performed using .01M solutions of $K_2[Ru(H_2O)Cl_5)$ (11) and $Na_2[PtCl_4]$ (Alpha), both in .1M Na_2SO_4, at potentials where H_2 was not observed even at a prolonged passage of current. Ru^{+3} was reduced to Ru at -.35V vs SCE and Pt^{+2} at -.30 V vs SCE in thicknesses of 5,10 and 15Å estimated from the measured current densities (.2 ma cm^{-2}) and the brief deposition times (several seconds).

Voltammograms measured immediately after deposition of the Ru showed no increase, and often a slight decrease, in photocurrents compared to those of naked electrodes. However, after rinsing and drying the treated electrodes, some increases in photocurrents were noted. Since just the measurement of the anodic waves passed more than sufficient

current (at potentials exceeding the required -.5V for Ru/RuO_2) to oxidize all the deposited Ru several times, it was inferred that the agent responsible for the enhancement was RuO_2, and not Ru^{+3} chemisorbed into the Fe_2O_3 lattice, an effect noted by Johnston, et al (12). In a few experiments the Ru deposited electrode was immersed for 5 sec in 10 M HNO_3 to oxidize the Ru. RuO_4, a second possible oxidized form of Ru, is volatile and produced only under extreme conditions (13). ESCA experiments were not successful in positively identifying this small amount of RuO_2, however.

The gases produced by each photoelectrode during photoelectrolysis were qualitatively identified using D_2O and H_2O^{18} enriched solvents and a UTI 100C Quadrapole Mass Spectrometer. HD and D_2 clearly formed during the photoelectrolysis catalysed by p-GaP, and $O^{16} - O^{18}$ and $O^{18}-O^{18}$ were easily observable during that by n-Fe_2O_3. Quantitatively a Varian Model 3700 Gas Chromatograph, with a 2m column of molecular sieve 5A, was used to check the gas yields. In addition, the pH in some unbuffered experiments changed in accordance with equations [1] and [2], as measured by a Corning 125 pH meter.

$$2H_2O + 2e^- \xrightarrow[h\nu]{\text{p-GaP}} H_2 + 2OH^- \qquad [1]$$

$$2H_2O \xrightarrow[h\nu]{\text{n-}Fe_2O_3} O_2 + 4H^+ + 4e^- \qquad [2]$$

Quantum yield measurements were made using the Reinecke salt method (14).

Results and Discussions

Figures 4 and 5 demonstrate the effect of trace depositions of Pt and RuO_2 on the photocurrents of the separate p-GaP and n-Fe_2O_3 electrodes. Table I summarizes these data for all electrodes in our study in terms of the voltage shift for half the maximum photocurrent ($\Delta V_{\frac{1}{2}}$), a crude measure of the effectiveness of the enhancement. It is also seen that the photocurrents near the onset potentials are small but the waves overlap in the region -.1 to +.1 V vs SCE, so that a combined short circuited unit would be predicted to pass some photocurrent even if with rather poor efficiency.

Table I. Photocurrent Enhancements of p-GaP and n-Fe_2O_3 Electrodes with Surface Catalysts.

p-GaP Electrode	Deposition Method	Estimated Pt Thickness (Å)	$\Delta V_{1/2}$ (volts)
2	vacuum	8	(- .10)
3	vacuum	11	+ .40
4	vacuum	14	+ .10
5	electrolysis	~5	+ .30
6	electrolysis	~10	+ .10
7	electrolysis	~15	+ .15

n-Fe_2O_3	Oxidation Method[a]	Estimated Ru Thickness (Å)	$\Delta V_{1/2}$ (volts)
2	HNO_3	~10	- .05
3	HNO_3	~10	- .10
4	HNO_3	~10	- .15
5	anodic	~5	- .10
6	anodic	~10	- .05
7	anodic	~15	(- .20)

[a]Deposited electrolytically.

These data plainly indicate enhanced photocurrents by the surface treatment of these semiconductors with trace amounts of known H_2 and O_2 generating catalysts. The $\Delta V_{\frac{1}{2}}$ values for Pt on p-GaP compare favorably with the ~ +.30V value of Nakato et al (15). Figure 6 demonstrates the effects of the surface catalysts on the photocurrents measured under bias. It is clear that a rather substantial (ca 3 fold) increase in photocurrent is observed for Pt treated p-GaP and that the photocurrent does not decay as fast with time. On the other hand, the RuO_2 enhancement is only temporary and the decay of the photocurrent may even be slightly accelerated over that of the naked n-Fe_2O_3 electrode. Thus, while the overall results of surface catalytic deposition are encouraging, more carefully controlled conditions of deposition and testing are needed to fully exploit this technique.

When the two photoelectrodes are combined in the electrochemical cell an interesting cooperative effect is noted. Figure 7 shows that the photocurrent obtained when both electrodes are illuminated is between 2-3 times the sum of the photocurrents measured when each is illuminated separately in the combined cell. Although this effect is produced under same bias, to allow the currents to be easily measured, it suggests that a similar enhancement may occur when no bias is applied, as in the combined monolithic unit.

This cooperative effect is somewhat clarified in Figure 8, which notes the position of the counter electrode (p-GaP) with respect to the working electrode (n-Fe_2O_3) at the turning point of the anodic scan. It is clear that illuminating p-GaP reduces the external bias necessary to obtain a given photocurrent from n-Fe_2O_3, while at the same time no shift of the anodic wave vs. SCE occurs. Thus illumination of p-GaP raises its Fermi level while leaving the polarization of the illuminated n-Fe_2O_3 undisturbed. This mutual enhancement may be understood if the dark counter electrode (p-GaP) is considered to be current limiting, since no majority carriers are being photo produced. Extra bias is then necessary to achieve the same current flow attainable when the p-GaP is

illuminated. The light on p-GaP produces both charge carrying ability (hence conductivity) and a photovoltage which complements the bias.

Figure 9 depicts a schematic view of the combined p/n heterodiode cell and a typical GC trace obtained when an aliquot of the vapor above the .1M Na_2SO_4 solution is injected onto the GC olumn. (The companion oxygen peak is not detectable at the levels corresponding to the amount of detected hydrogen.) When combined with the intensity of incident photons it is possible to estimate a H_2 quantum yield of between .02 and .1, depending upon how much H_2 is assumed to remain dissolved. A control dark reaction produced no detectable H_2. The corresponding yield from seawater, using natural solar radiation, is an order of magnitude less than that measured using .1M Ma_2SO_4 as an electrolyte, and this dimunition of yield is continued even when .1M Ma_2SO_4 is restored as the electrolyte. Thus it appears that seawater photoelectrolysis may irreversibly damage the cell, perhaps involving the oxidation of Cl^- instead of H_2O.

Table 2 combines the p/n heterodiode data now available. It is seen that the present configuration compares relatively favorably in yield, considering that two visible light band-gap semiconductors, one of which is made of a polycrystalline material, are used. The use of close to neutral pH electrolytes is perhaps superfluous at the present state of development of these cells, but it seems important to demonstrate that a practical system will probably not involve the addition of large quantities of concentrated acids or bases to water to enable photoinduced water splitting.

Conclusion

A p/n heterotype photochemical diode, consisting of polycrystalline n-Fe_2O_3 and Zn-doped p-GaP has been shown to split water using visible light with a low quantum efficiency. Surface catalysts of RuO_2 and Pt, on the anode and cathode respectively, can enhance the observed photocurrents, the former only temporarily, however. Photoelectrolysis of seawater producing hydrogen has also been accomplished with natural solar radiation using this cell.

Table 2. Summary of p/n Photochemical Diode Date

Anode	Anode Absorption	Cathode	Cathode Absorption	Electrolyte	Efficiency (%)	Reference
n-TiO_2	uv	p-GaP	vis	1 N H_2SO_4	-	3
n-GaP	vis	p-GaP	vis	.2 N H_2SO_4	(unstable)	4a
n-TiO_2	uv	p-GaP	vis	.2 N H_2SO_4	.25	4a
n-TiO_2	uv	p-CdTe	ir	1 N NaOH	.044	5
n-TiO_2	uv	p-GaP	vis	1 N NaOH	.098	5
n-$SrTiO_3$	uv	p-CdTe	ir	1 N NaOH	.18	5
n-$SrTiO_3$	uv	p-GaP	vis	1 N NaOH	.67	5
n-Fe_2O_3†	vis	p-GaP	vis	.1 Na_2SO_4	.02-.1	present
n-Fe_2O_3†	vis	p-GaP	vis	seawater	.002-.01	present

† Polycrystalline. Other materials are single crystals.

Acknowledgements

This work was supported by the Office of Basic Energy Sciences, Division of Chemical Sciences, of the United States Department of Energy under contract W-7405-Eng-48. Howard Mettee wishes to thank Youngstown State University for partial support during his Faculty Improvement Leave.

The enthusiastic assistance of Mr. Steve Gest in performing many of the electrochemical measurements is deeply appreciated, as is the help of the Vacuum Coating Department of the Lawrence Berkeley Laboratory.

References

1. A. Fujishima and K. Honda, Nature 238 (1972) 37.

2. (a) M. Wrighton, Accts. Chem. Res. 12 (1979) 303; (b) A.J. Nozik, Ann. Rev. Phys. Chem. 29 (1978) 189.

3. H. Yoneyama, H. Sakamoto and H. Tamura, Electrochim. Acta 20 (1975) 341.

4. (a) A.J. Nozik, App. Phys. Letts 29 (1976) 150; (b) ibid. 30 (1977) 567.

5. K. Ohashi, J. McCann and J. O'M. Bockris, Nature 266 (1977) 610.

6. (a) K.S. Yun, S.M. Wilhelm, S. Kapusta and M. Hackerman, J. Electrochem. Soc. 127 (1980) 85; (b) S.M. Wilhelm, K.S. Yun, L.W. Ballenger and N. Hackerman, J. Electrochem. Soc. 126 (1979) 420.

7. M.A. Butler and D.S. Ginley, J. Electrochem. Soc. 127 (1980) 1273, and references cited therein.

8. H. Gerischer, Electroanal. Chem. and Interfac. Electrochem. 58 (1975) 263.

9. L.R. Yeh and N. Hackerman, J. Electrochem. Soc. 124 (1977) 833.

10. J.F. Hamilton and R.C. Baetzold, Science 205 (1979) 1213.

11. T.D. Avtokratora, "Analytical Chemistry of Ruthenium", Humphrey Science Publishers, Ann Arbor (1969) 217.

12. W.D. Johnston, Jr., H.L. Leamy, B.A. Parkinson, A. Heller and B. Miller, J. Electrochem. Soc. 127 (1980) 90.

13. W.M. Latimer, "Oxidation Potentials", 2nd ed., Prentice Hall, New York (1952).

14. E.E. Wegner and A.W. Adamson, J. Amer. Chem. Soc. 88 (1966) 394.

15. Y. Nakato, S. Tonomura and H. Tsubomura, Ber. Bunsenges Phys. Chem. 80 (1976) 1289.

16. J. Kennedy and K.W. Frese, J. Electrochem. Soc. 125 (1978) 732.

Figure Captions

Figure 1. The light absorbing and charge separating functions of natural photosystems I and II, in addition to the water redox reactions, are artificially duplicated by p- and n-type semiconductors.

Figure 2. The dark equilibrium energetics of the n-Fe_2O_3/p-GaP photochemical diode at pH = 7 shows a disposition of the valence band of n-Fe_2O_3 and the conduction band of p-GaP sufficient to oxidize and reduce water, respectively. (Date from (2) and (16).)

Figure 3. The photoelectrochemical apparatus used to characterize individual semiconductor electrodes before and after deposition of trace amounts of Pt on p-GaP and RuO_2 on Fe_2O_3.

Figure 4. Current-voltage curves of a p-GaP electrode before (I) and after (II) vacuum deposition of ca. 11 Å Pt. Scanning rate: ~50 mV/sec. Pt mesh is the counter electrode.

Figure 5. Current-voltage curves of an n-Fe_2O_3 electrode before (I) and 12 hrs. after (II) electrolytic deposition (and subsequent oxidation) of 5 Å Ru. Curve (III) was measured after a 30 min "aging" experiment which passed .65 coulomb with electrode poised at 1.05 V vs. SCE. Scanning rate: ~50 mV/sec. Pt mesh is the counter electrode.

Figure 6. Upper: Photocurrent vs. time of a p-GaP electrode before and after vacuum deposition of ca. 11 Å Pt; lower: photocurrent vs. time of an n-Fe_2O_3 electrode before and after electrolytic deposition (and subsequent oxidation) of 5 Å Ru.

Figure 7. Photocurrents of combined p/n heterodiode system, with n-Fe_2O_3 as the working electrode and p-GaP as the counter electrode. The trace begins in the dark with 0 bias(1); increasing the bias to 1.6 V moves WE to .33 V (2); illuminating only p-GaP shifts WE to .8 V (3), illuminating only n-Fe_2O_3 shifts WE to 0 (4); illuminating both electrodes simultaneously shifts WE to .35 V (5).

Figure 8. Current-voltage curves of n-Fe_2O_3 as working electrode and p-Gap as counter electrode. The photovoltage of p-GaP does not disturb n-Fe_2O_3 vs. SCE but instead shifts p-GaP .7 V so that less external bias is required to sustain the same current.

Figure 9. The combined p-GaP/n-Fe_2O_3 heterophotochemical diode on the same side of an insulated pure Fe plate, with a GC trace showing H_2 (above the background signal) obtained when the cell is illuminated with sunlight in .1M Na_2SO_4 for 5 hours.

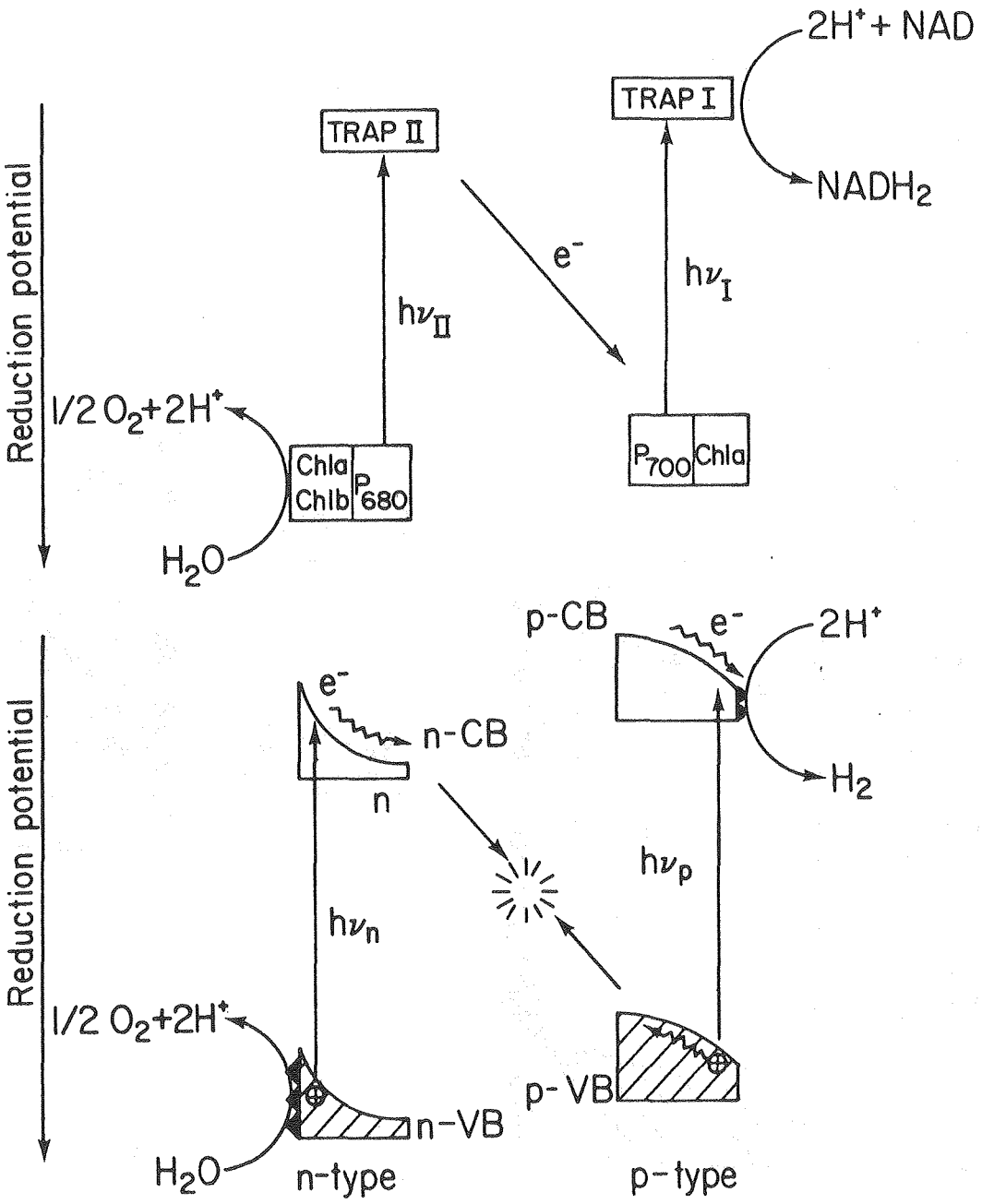

XBL 808-4326

"Figure 1, Mettee et al"

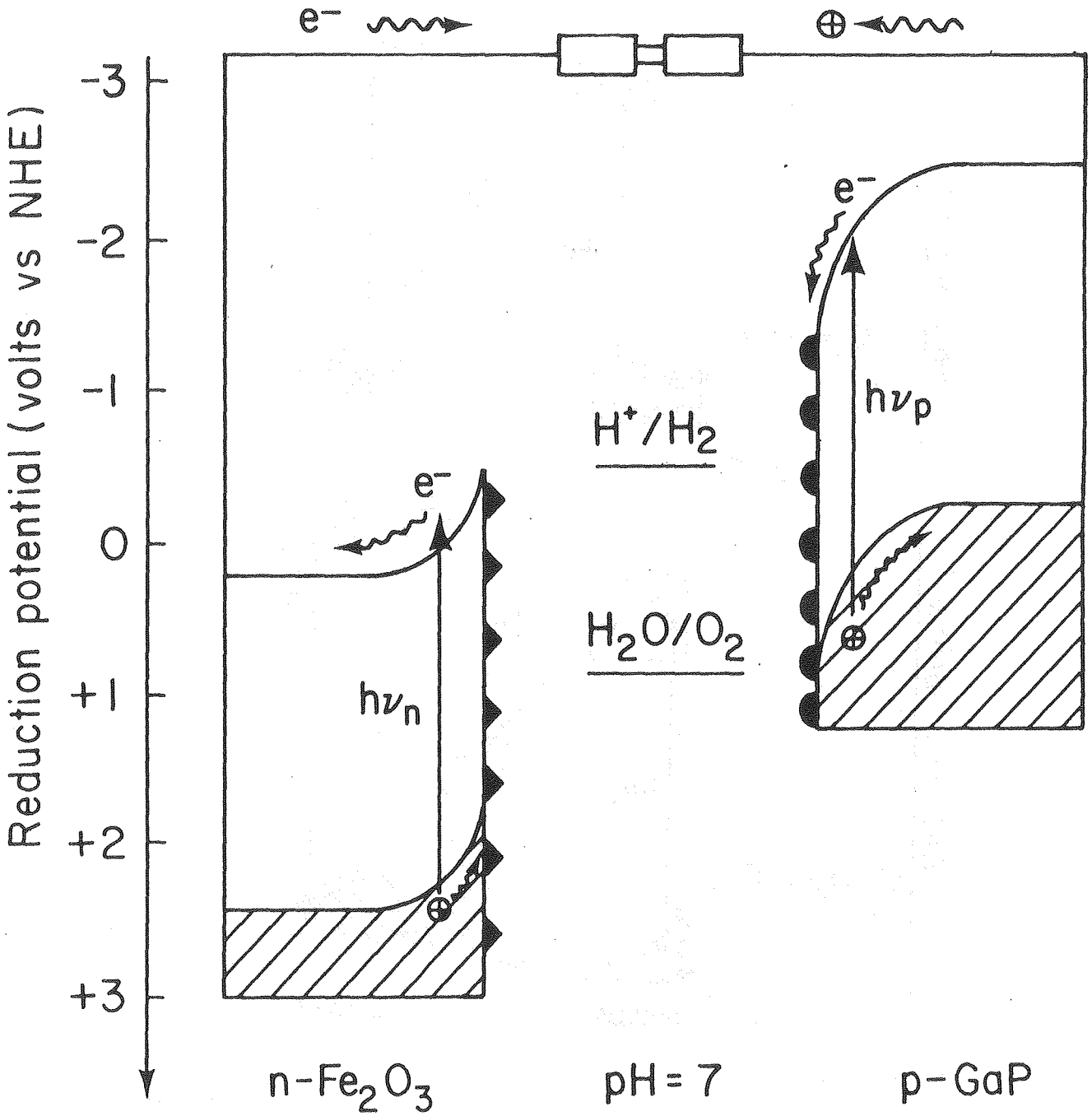

XBL 808-4325

"Figure 2, Mettee et al"

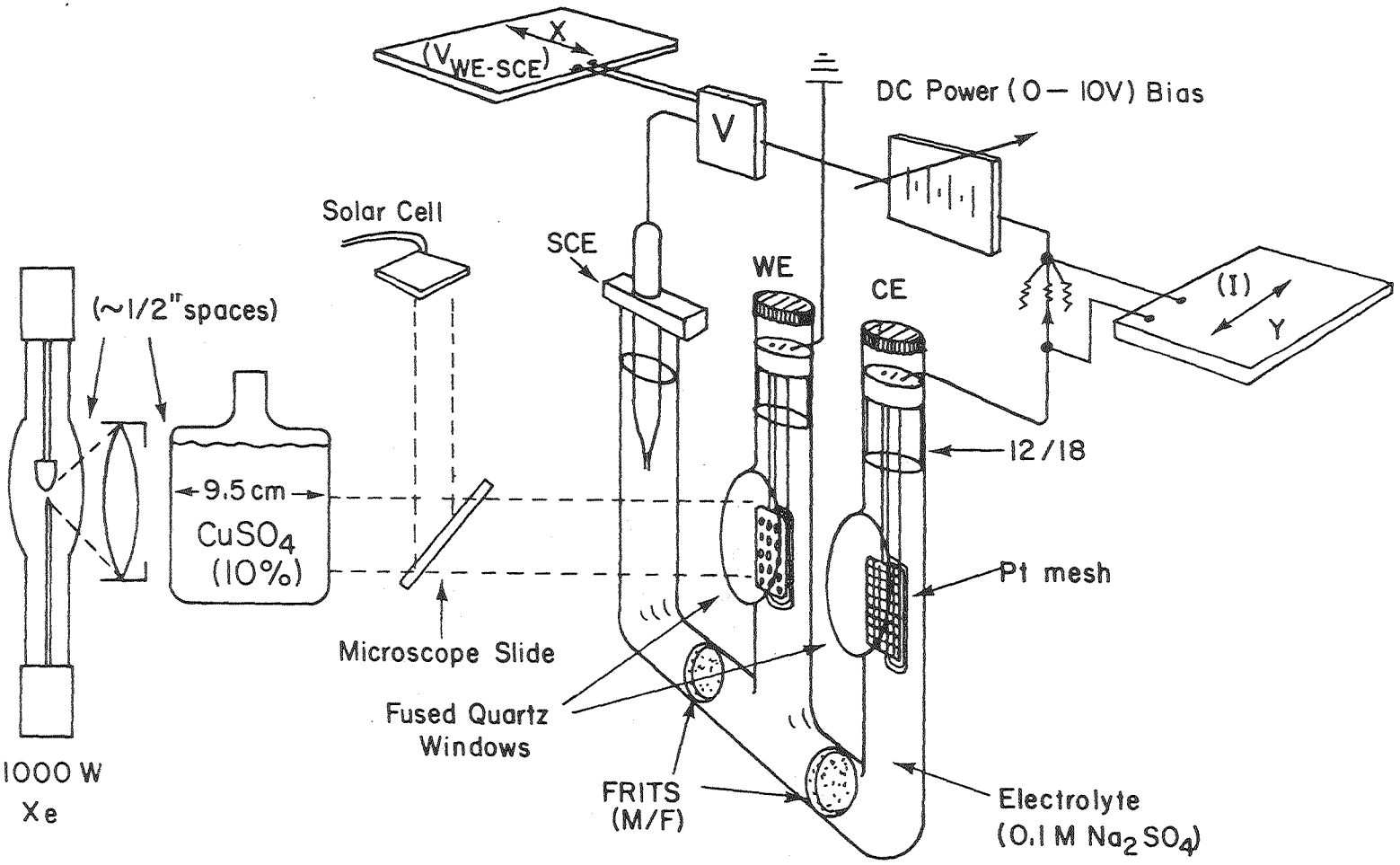

XBL 808-4327

"Figure 3, Mettee et al"

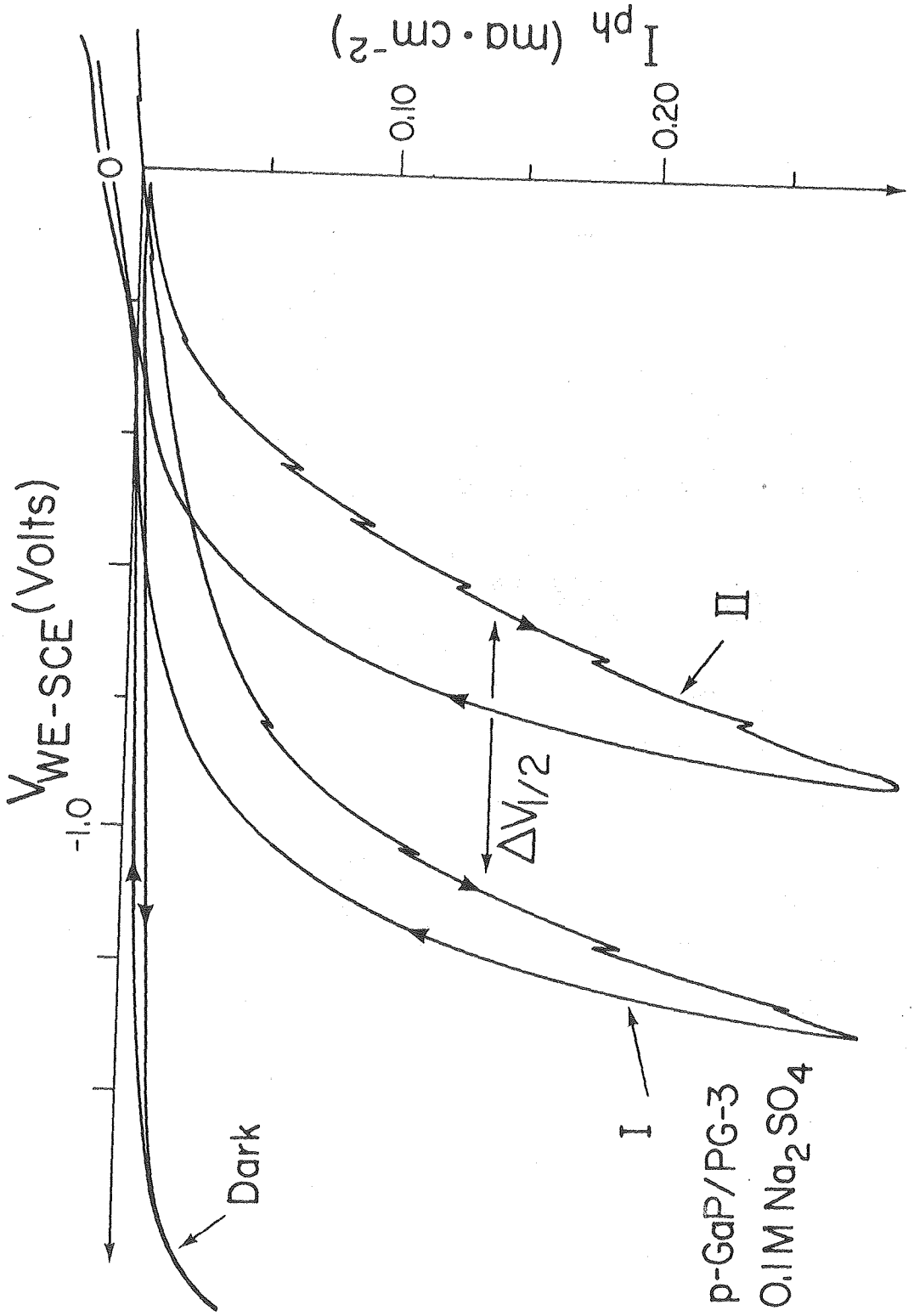

"Figure 4, Mettee et al"

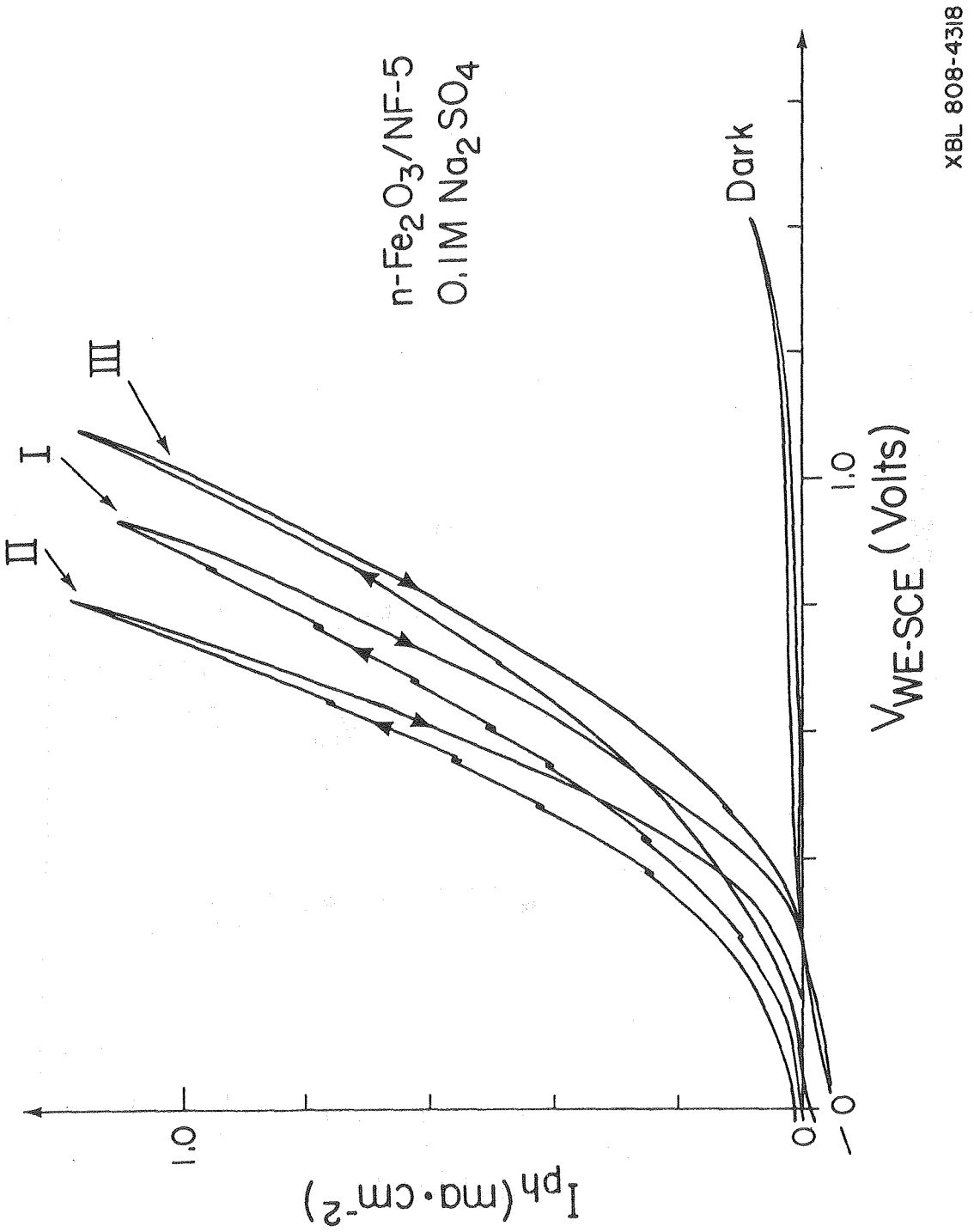

"Figure 5, Mettee et al"

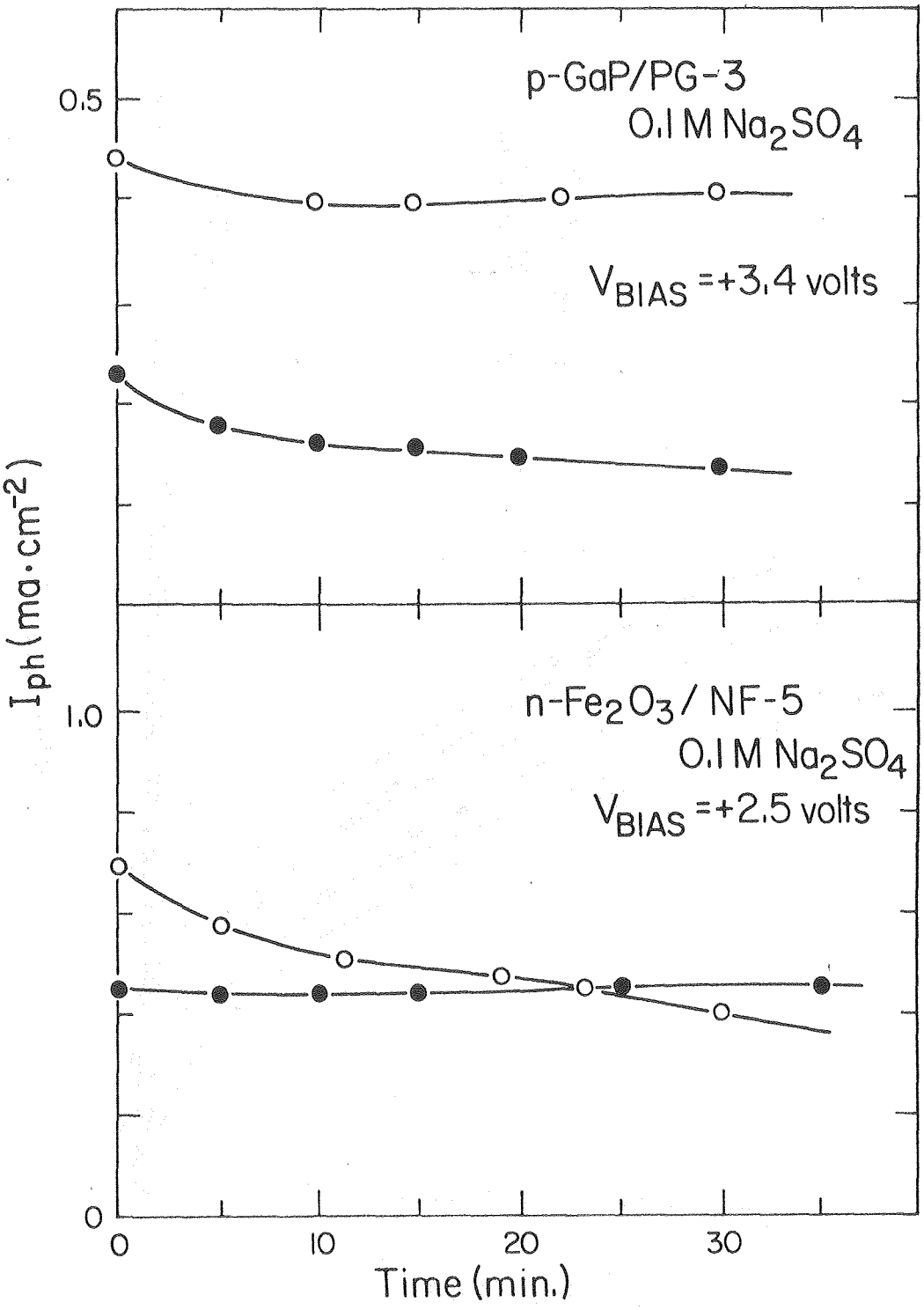

XBL 808-4323

"Figure 6, Mettee et al"

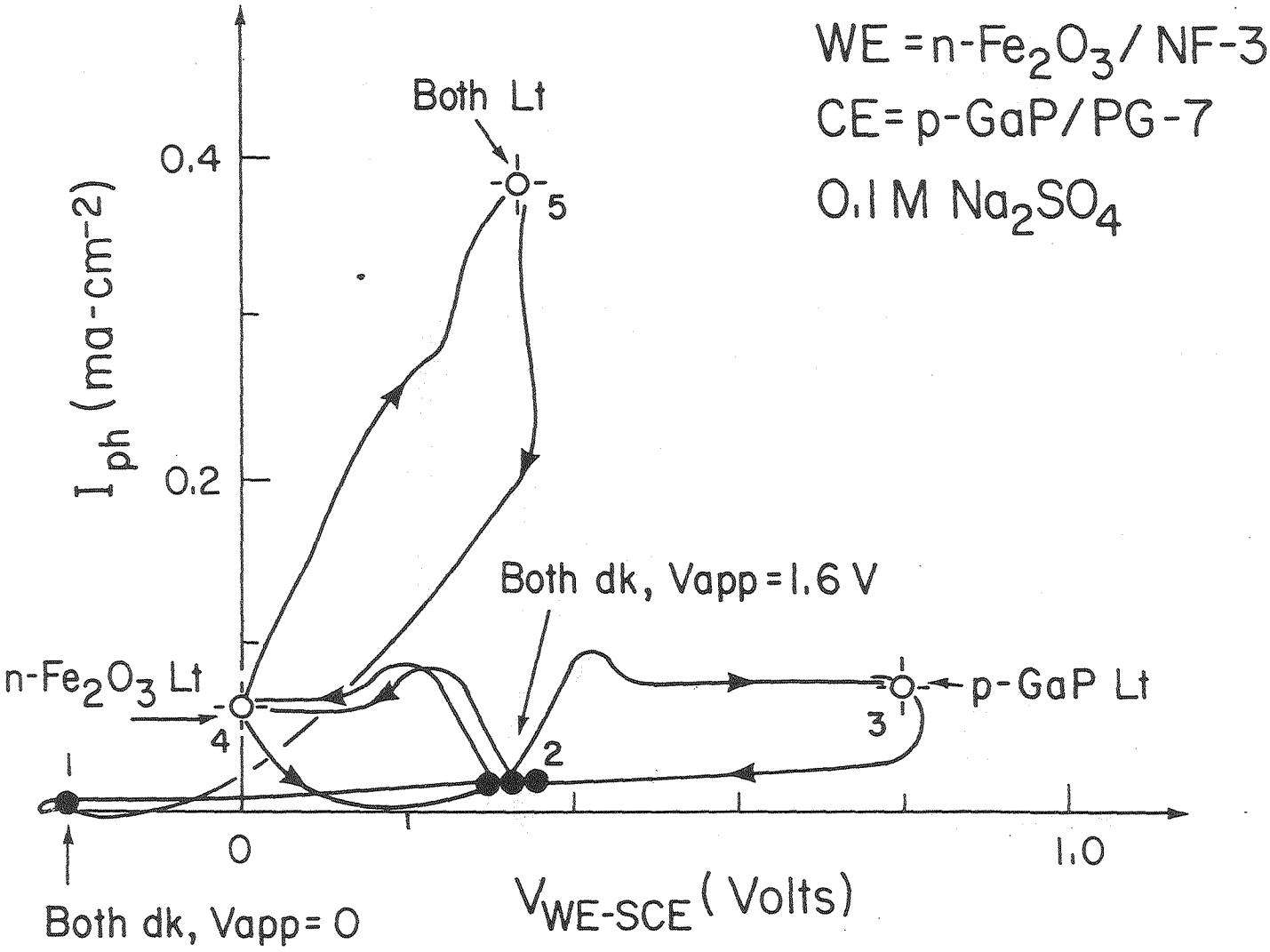

XBL 808-4319

"Figure 7, Mettee et al"

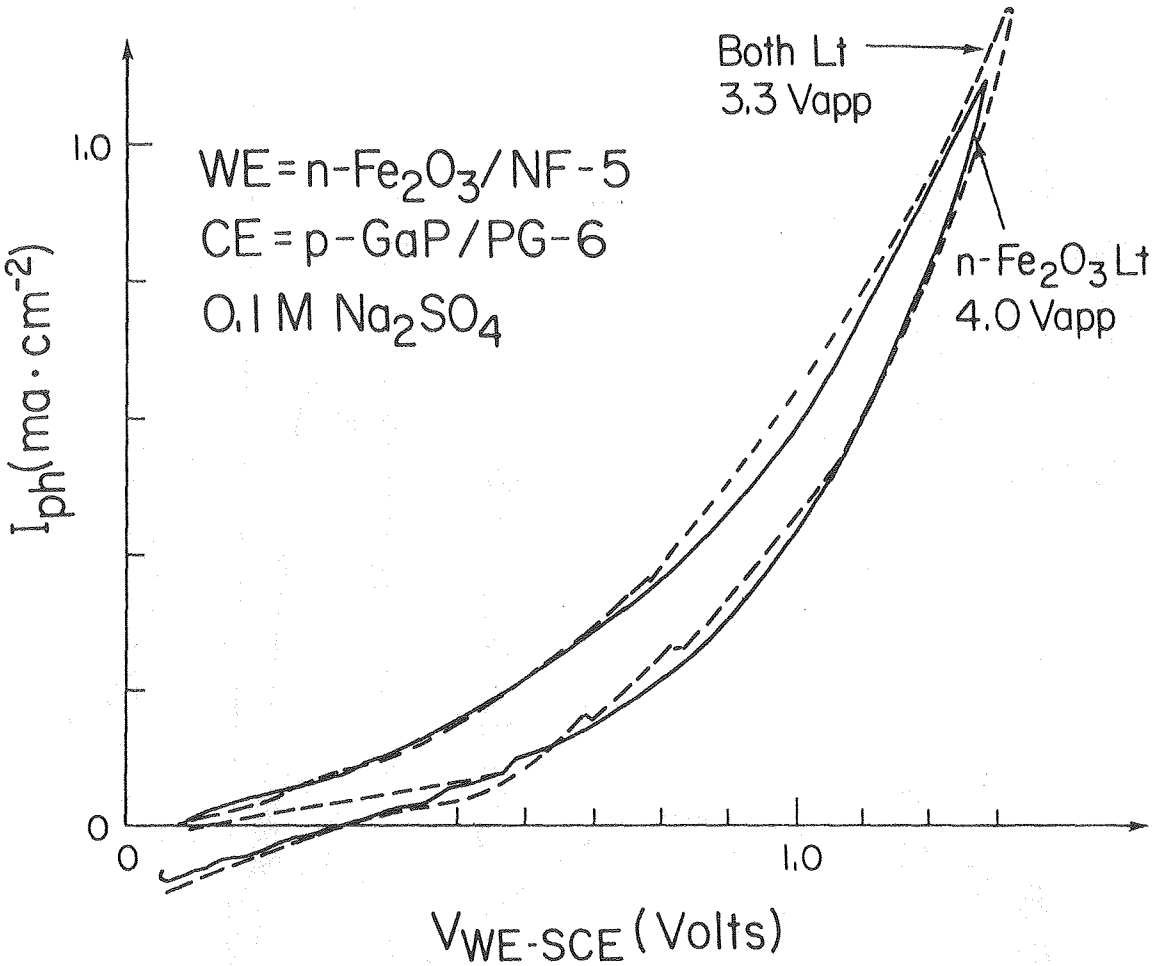

XBL 808-4322

"Figure 8, Mettee et al"

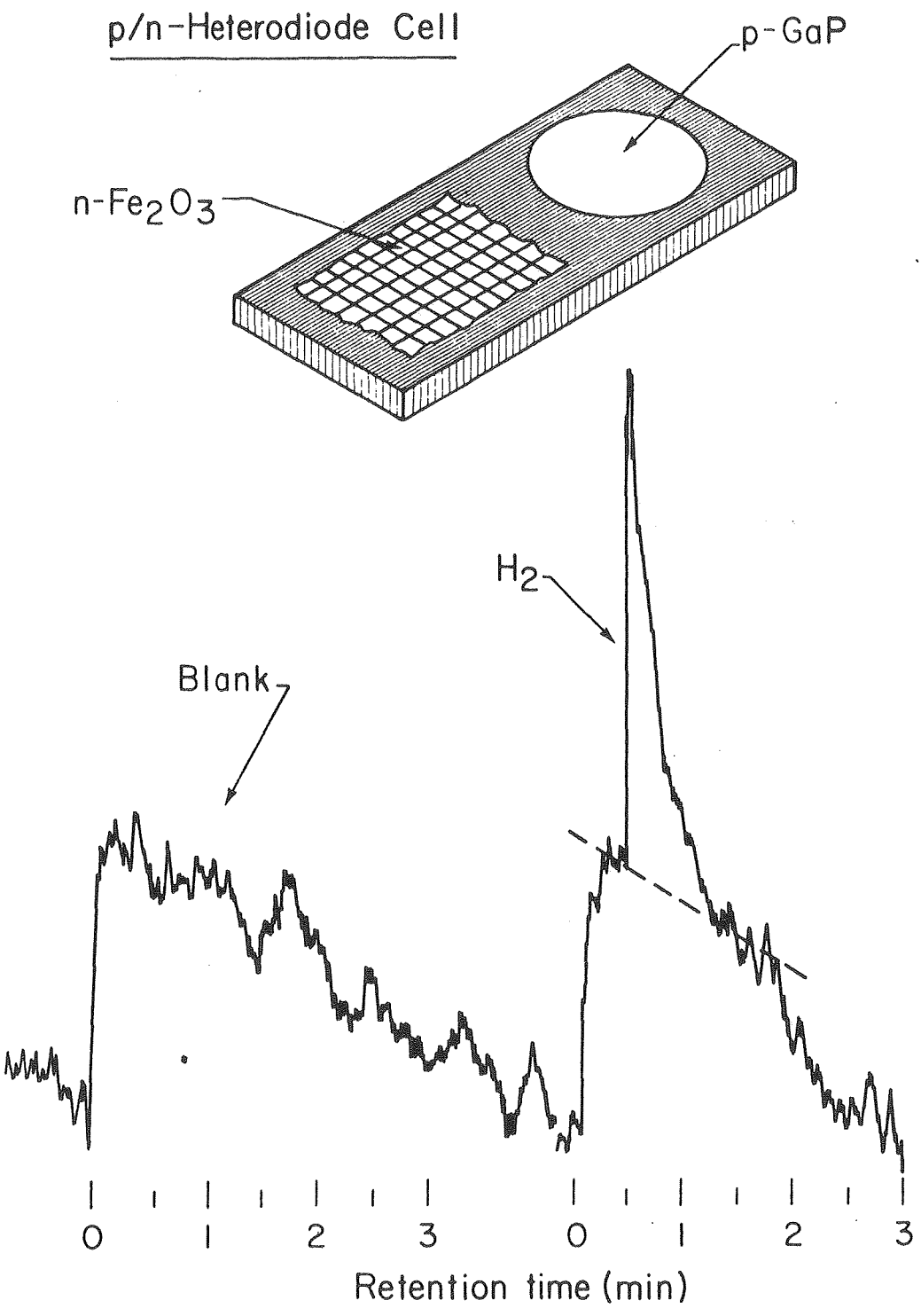

XBL 808-4324

"Figure 9, Mettee et al"